3D CFD ANALYSIS OF HEAT TRANSFER IN A SCRAPED SURFACE HEAT EXCHANGER FOR BINGHAM FLUIDS

Ali S.* and Baccar M.
*Author for correspondence
Department of Mechanical Engineering,
National Engineering School of Sfax,
Sfax, 3038,
Tunisia,
E-mail: sirineali@ymail.com

ABSTRACT

This study is focused on numerical analysis of the thermal behavior within a scraped surface heat exchanger (SSHE) for threshold fluids (Bingham fluids). An innovative SSHE is considered which includes helical ribbon, instead of using scrapers. Heat transfer simulations were carried out by means of specific CFD code to solve the three dimensional form of continuity, momentum and energy equations. In this work, the influence of dimensionless numbers (rotational Reynolds, axial Reynolds and Oldroyd numbers) on thermal behavior is studied. Numerical results show that for low axial Reynolds numbers compared to rotational Reynolds number (Reax/Rer <1), there is opposition between the axial components of velocity coming from the flow (ascending components) and axial components at the helical ribbon due to the mixing effect (descending components). However, for high axial Reynolds numbers (Re_{ax}/Re_r >1), a parabolic-like flow is generated, indicating low degree of back mixing. Numerical results show also that an important heated zone was observed near the blades due to high blades rotating speed. The highest temperatures are found at the thermal boundary layer periodically disturbed by the helical ribbon. It appears that increasing the Oldroyd number produces a slight rise in the temperature field.

INTRODUCTION

Scraped Surface Heat Exchanger (SSHE) is a device used in processing highly viscous and sticky products which are mostly found in food and chemical industries. Problems such as fouling and back mixing phenomenon can occur, and causes decreasing of the overall heat transfer coefficient. One of the several solutions consists of replacing the rotating blades found in the commercial practices by helical ribbon.

Studying heat transfer within SSHE was the interest of many researchers; Baccar and Abid [1] have conducted ~~did~~ a 3D numerical simulation in order to analyse the hydrodynamic and thermal behaviour under different geometrical and operating conditions. M. Örvös et al. [2] gave an experimental study in order to determine a heat transfer equation by varying different operational parameters. Ben Lakhdhar et al. [3] established the influence of many parameters on heat transfer which are: product type and composition, blade rotation speed, flow rate and distance between blades and wall. They carried out an experimental study on SSHE used for freezing of water-ethanol mixture and aqueous sucrose solution and they found two correlations one for the ethanol, and the other for the sucrose. Martinez et al. [4] created an innovative heat exchanger which is mechanically assisted by a reciprocating cylinder, they analysed the flow pattern and pressure drop mechanisms in static and dynamic conditions. Yataghene et al. [5] achieved a 3D-numerical modelling to examine the thermal performance of a SSHE for Newtonian and non-Newtonian fluids with varying blades speed and mass flow rate. Boccardi et al. [6] developed two heat transfer correlations for a SSHE using experimental data, they used for the first one the dimensionless geometrical number D/L, and for the second one a new number which considers other agitator characteristics.

SSHE consists of: stator which is the heat exchanger surface with the fluid, rotor which contains rotating blades in order to prevent crust formation by scraping the exchanger surface (see figure 1).

This study presents an innovative SSHE which, instead of using scraping blades, is assisted by helical ribbon. Three-dimensional numerical simulations of Bingham fluids are performed in order to understand the influence of the helical ribbon on hydrodynamic and thermal behaviors within SSHE.

NOMENCLATURE

C_p	[J/kgK]	Specific heat of the fluid
D	[m]	Internal diameter of the exchanger
d_a	[m]	Agitator diameter
d_r	[m]	Rotor shaft diameter
h	[W/m^{2}K]	Heat transfer coefficient
L	[m]	Length of the exchanger
N	[rev/s]	Rotational speed
P	[Pa]	Pressure
p	[-]	Pitch of the helical ribbon
R	[m]	Internal exchanger radius
r	[m]	Rotor shaft radius
T	[K]	Temperature
U,V,W	[m/s]	Velocity components
r,θ,z	[-]	Coordinates system

Special characters

ρ	[Kg/m^3]	Fluid density
λ	[W/mK]	Thermal conductivity of air
μ	[Pa.s]	Dynamic viscosity

η	[-]	Apparent viscosity
ν	[m²/s]	Kinematic viscosity

Subscripts

In	Inlet
Out	outlet
W	wall

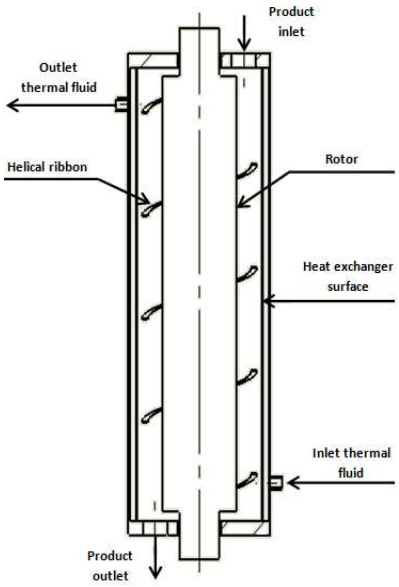

Figure 1 Schematic representation of a SSHE with helical ribbon

NUMERICAL MODEL

Geometry and mesh

A specific CFD (Computational Fluid Dynamics) code was used in the simulation of the hydrodynamic and thermal behaviors, based on the Finite Volume Method (FVM). The methods of discretization used for the modeling of velocity and temperature fields were the hybrid scheme and the exponential scheme, respectively. The grid size used in the simulation is 230400 computational cells (36 in the radial, 40 in the tangential and 160 in the axial direction). The ratio of rotor shaft radius to internal exchanger radius (r/R) is equal to 0.6. The ratio of exchanger height to its internal radius (H/R) is equal to 6. This configuration is the same as that studied experimentally by Trommelen and Beek (1971) [7] and numerically by Baccar and Abid (1997) [1].
The helical ribbon extends over four pitches (see figure 1). It was driven by the rotor, to continuously scrape the stator wall.
The method of discretization used for the modeling was the hybrid scheme. The grid size used in the simulation is 230400 computational cells (36 in the radial, 40 in the tangential and 160 in the axial direction).

Governing equations

In this section the conservation equations of continuity, momentum and energy have been solved basing on the Finite Volume Method (FVM). The flow is considered steady, laminar, non-isothermal, and incompressible.

The continuity equation for the velocity in the rotating reference frame is written as:

$$\operatorname{div} \vec{V} = 0 \tag{1}$$

With $\vec{V}$ is the velocity vector.
The momentum equation can be expressed in the tensorial form as follows:

$$\rho\left(\frac{\partial \vec{V}}{\partial t}+\overrightarrow{\operatorname{grad}\vec{V}}.\vec{V}\right)=-\overrightarrow{\operatorname{grad}P}+\operatorname{div}\vec{\vec{\tau}}+\rho\vec{g} \tag{2}$$

The tensorial strain can be written considering a purely viscous generalized Newtonian fluid:

$$\vec{\vec{\tau}}=\eta\left|\dot{\gamma}\right| \tag{3}$$

Where $\dot{\gamma}$ is the shear rate, and η is the apparent viscosity.

In a rotating frame, Centrifugal and Coriolis acceleration which defined respectively as $-w^2.\vec{r}$ and $2\vec{w}\wedge\vec{r}$ were added to the momentum equation.

The conservation equation of energy is expressed as:

$$\rho C_p\frac{\partial T}{\partial t}=-\operatorname{div}\left(-\lambda\overrightarrow{\operatorname{grad}T}+\rho C_p\vec{V}T\right) \tag{4}$$

BOUNDARY CONDITIONS

The fluid enters the exchanger with an axial constant velocity:

$$W_{inlet} = \text{constant} \tag{5}$$

In the region where the fluid exits the computational domain, the velocity gradient equals to zero:

$$\frac{\partial W_{outlet}}{\partial z}=0 \tag{6}$$

The presence of the rotor and helical ribbon was taken into account. Thus, all radial and tangential velocity mesh nodes which intersect with the rotor or the ribbon were taken equal to zero. The angular velocity component, at the internal wall exchanger, equal to the rotating speed because of the rotating frame. Thus, the dimensionless angular velocity is imposed equals to -1.

The boundary conditions of the temperature field are taken as follows: the temperature at the entrance of the exchanger is constant that's why the dimensionless temperature equals to zero. At the outlet of the exchanger and across the rotor the heat flux is zero (adiabatic wall). The dimensionless wall temperature equals to 1, and the derivative of dimensionless temperature relative to z equals to 0.

$$\theta_{in} = 0$$
$$\theta_w = 1 \qquad (7)$$
$$\frac{\partial \theta}{\partial z} = 0$$

REHOLOGICAL MODEL

High viscous and non-Newtonian products were treated in SSHEs. For solving momentum equation, there are many mathematical models that describe the rheological behavior, where the apparent viscosity (η) is a non-linear function of the shear rate ($\dot{\gamma}$). Many of fluid materials have a yield stress, a critical value of stress below which they do not flow; they are called viscoplastic materials or Bingham plastics.

In this study, the model of Papanastasiou was considered who suggested an exponential regularization of the Bingham model, by introducing a parameter m, which controls the exponential growth of stress [8].

The proposed model, called also Bingham-Papanastasiou model, has the following form:

$$\eta = 1 + \frac{Od\left[1 - \exp\left(-m|\dot{\gamma}|\right)\right]}{|\dot{\gamma}|} \qquad (8)$$

The viscoplastic character of the flow is assessed by a Bingham number (Bn) or Oldroyd number (Od), defined by:

$$Bn = Od = \frac{\tau_y D}{\mu V_a} \qquad (9)$$

Where τ_y is the yield stress and V_a is the average velocity of the viscoplastic fluid.

In the case of Bn = Od= 0, the fluid is Newtonian. However, at the other extreme (Bn = Od tends to infinity) the fluid is unyielded solid.

RESULTS AND DISCUSSION

The effect of Oldroyd on velocity and thermal fields was described in this paragraph. Also, a representation of the rigid zones was given.

Hydrodynamic behaviour

Figure 2 shows the non-dimensional velocity distribution in a (r-z) plane. It illustrates the influence of the Oldroyd number on the velocity distribution; it shows that when increasing the Oldroyd number the recirculation fluid zone becomes more reduced, for example the recirculation zone is near to disappear for Od=50.

The flow has an oscillatory path; when the helical ribbon hits the fluid every p/2 distance, it causes a deviation of the flow towards the regions not affected by the blockage. This deviation generates a local velocity increase, that's why a recirculation zone appears in the tip regions of the ribbon which has the most intensive hydrodynamic activity in the exchanger.

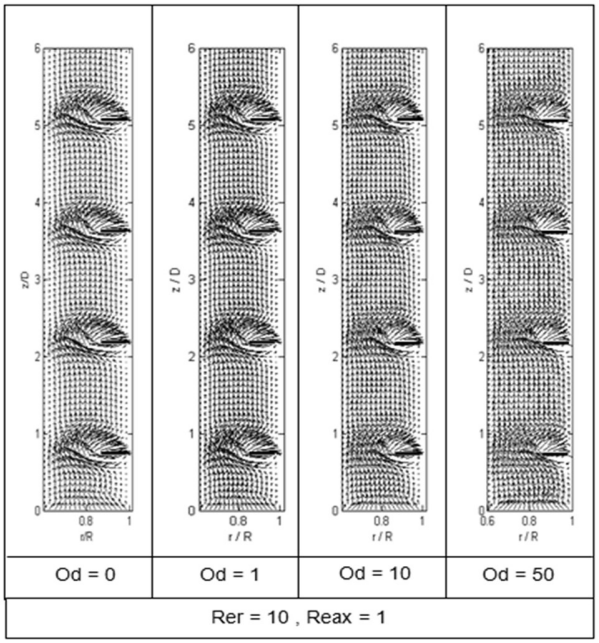

Figure 2 Flow behavior for different Oldroyd number

Rigid Zones

The rigid zones for different Oldroyd numbers are represented in (r-z) and (r-θ) planes respectively as shown in figure 3 and 4. They indicate that the highest values of shear rates are situated in the zone between the tip of the ribbon and the stator wall. Table 1 gives an idea about the percentage of rigid zones in the SSHE for different Od.

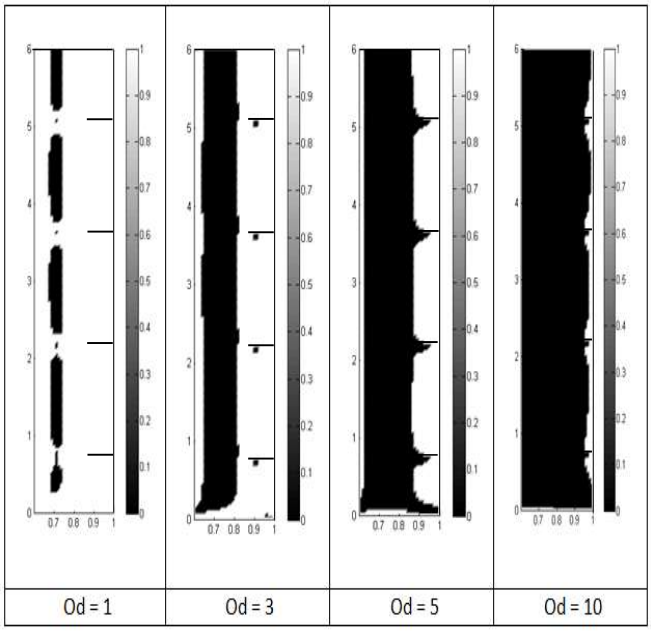

Figure 3 Rigid zones for different Od in (r-z) plane (Re_r=10; Re_{ax}=1).

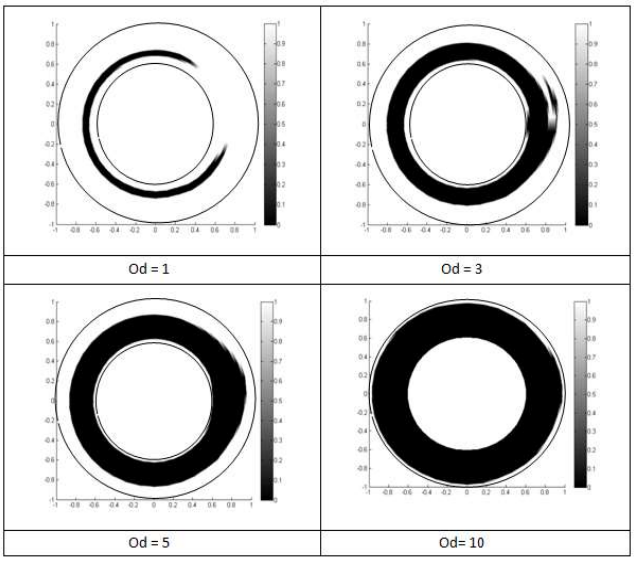

Figure 4 Rigid zones for different Od in (R-θ) plane (Re_r=10; Re_{ax}=1).

The total volume = 12.062 m^3				
Od	**1**	**3**	**5**	**10**
Volume of the rigid zones	1.242	4.872	7.443	10.958
% of unmixed volume	10.299%	40.391%	61.707%	90.848%
% of the mixed volume	89.7%	59.608%	38.292%	9.151%

table 1 Rigid zones within SSHE for different Od

Temperature Field

Figure 5 to figure 7 show examples of obtained numerical results for the temperature field in (r-z) plane inside SSHE. Important heated zones were observed near the helical ribbon due to the high rotating speed in these regions. The highest temperatures are found at the thermal boundary layer in all considered cases.

When the rotational Reynolds number increases, the heated zones become more important due to the mixing effect (see figure 5).

Figure 6 shows the effect of Re_{ax} on the thermal behavior for Od=1 and Re_r=10. Increasing the Re_{ax} means increasing the flow rate which leads to ameliorate the heat transfer. However, for low value of axial Reynolds numbers, the exit temperature of the fluid is manifestly higher, firstly because the back mixing becomes more important and secondly because the residence time of fluids within the SSHE is longer.

It appears, in figure 7, giving the thermal behaviors for different Od number, that the increase of Od slightly ameliorate the thermal behavior.

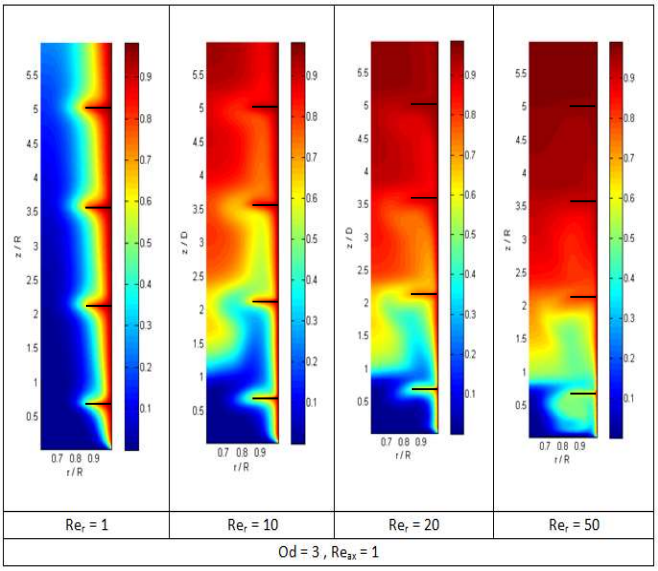

Figure 5 thermal behaviors for different Re_r

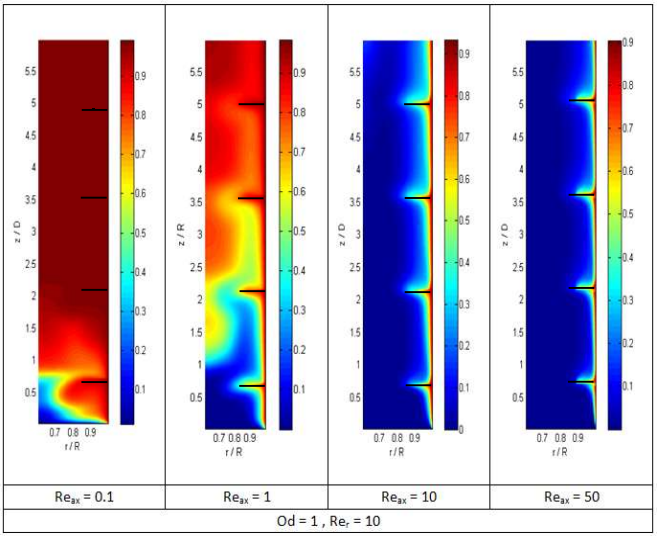

Figure 6 Thermal behaviors for different Re_{ax}

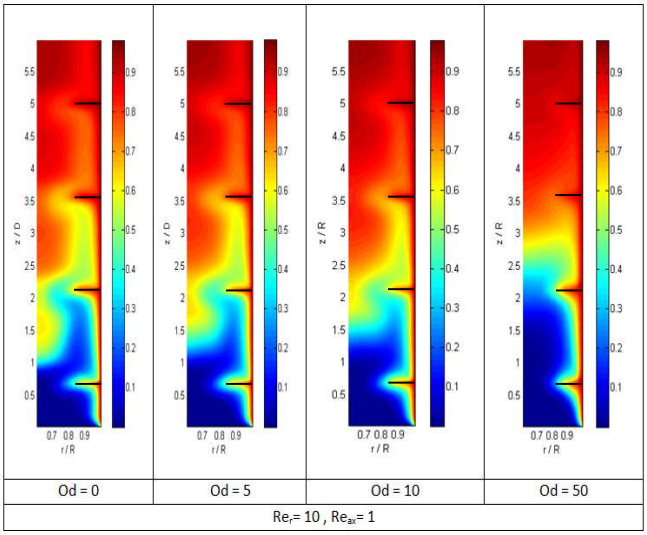

Figure 7 Thermal behaviors for different Od

Effect of Re_r and Re_{ax} on the Nusselt number

In Figure 8, the impact of two non-dimensional numbers on the Nusselt number is studied for Od = 3. Numerical results show that for low Reynolds numbers ratio ($\frac{Re_{ax}}{Re_r}$ <1), there is opposition between the axial components of velocity coming from the flow (ascending components) and axial components at the helical ribbon due to the mixing effect and the back-mixing phenomenon (descending components). However, for high Reynolds numbers ratio ($\frac{Re_{ax}}{Re_r}$ > 1), the conjugated effect of axial and rotational Reynolds numbers give upward flow behaviour.

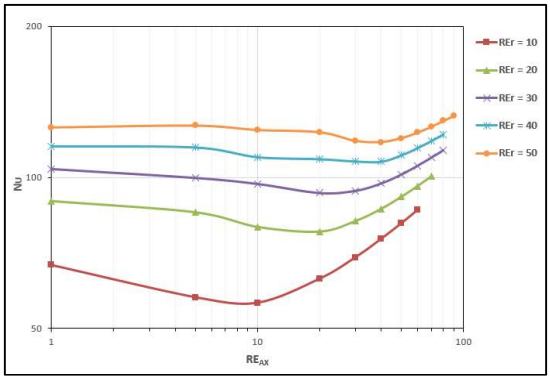

Figure 8 Nusselt number evolution with Re_{ax} for different Re_r

Comparison with anterior results

Numerical simulations were carried out in order to compare our numerical results with experimental values. It is noted that the effect of the axial Reynolds number is often neglected in previous correlations. Figure 9 is a log-log plot of Nusselt number (Nu) as a function of rotational Reynolds number (Re_r). A good agreement is revealed with anterior work of Maingonat and Corrieu who use in their study 4 row of blades.

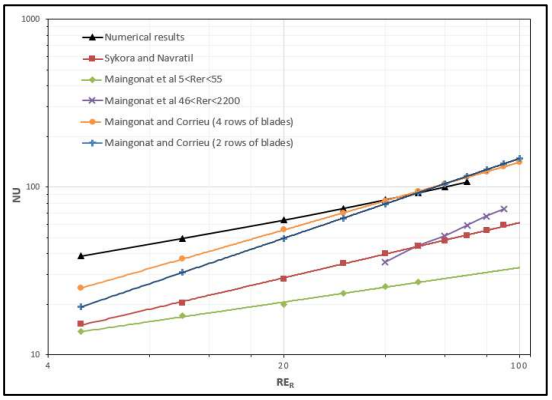

Figure 9 thermal behaviors for different Od

CONCLUSION

Numerical results indicate that increasing the rotating Reynolds, the axial Reynolds and Oldroyd numbers can improve the heat transfer. It was found that when the Od number increases, the rigid zones become more extended. The influence of Re_{ax} and Re_r on the Nusselt number shows that when rotating Reynolds number is bigger than the axial one, there is back-mixing phenomenon which leads to reduce the Nusselt number.

A heat correlation prediction using the dimensionless numbers: Re_r, Re_{ax} and Od numbers will be given afterwards.

REFERENCES

[1] Baccar M., and Abid M.S., Numerical analysis of three-dimensional flow and thermal behaviour in a scraped-surface heat exchanger, *Rev Gen Therm,* 1997, pp. 36, 7826790

[2] Örvös M., Balazs T., Both K.F., and Csury I., Investigation of heat transfer conditions in scraped surface heat exchanger, *Periodica Polytechnica Ser. Mech. Vol. 98, Nos. 2-9,* 1994, pp. 129-198

[3] Ben Lakhdar M., Cerecero R., Alvarez G., Guilpart J., Filck D., and Lallemand A., Heat transfer with freezing in a scraped surface heat exchanger, *Applied Thermal Engineering 25,* 2005, pp. 45-60

[4] Martinez D.S., Solano J.P., Pérez J., and Viedma J., Numerical investigation of Non-newtonian flow and heat transfer in tubes of heat exchangers with reciprocating insert devices, frontiers in heat and mass transfer (FHMT), 2, 033002, DOI: 10.5098. v2.3.3002, 2011

[5] Yataghene M., and Legrand J., A 2D-CFD model thermal analysis within a scraped surface heat exchanger, *Computers & Fluids 71*, 2013, pp. 380-399

[6] Boccardi G., Celata G.P., Lazzarini R., Saraceno R., and Trinchieri R., Development of a heat transfer correlation for a scraped-surface heat exchanger, *Applied Thermal Engineering 30*, 2010, pp. 1101-1106

[7] Trommelen A., Beek W. (1971), Phenomena in scraped-surface heat exchanger, *Chem. Eng. Sci.* 26, 1933

[8] Mitsoulis E. Flows of viscoplastic materials: models and computations. *Rheology Reviews,* 2007, pp. 135-178